Available online at www.sciencedirect.com
SCIENCE DIRECT
Journal of Power Sources 145 (2005) 124–132
JOURNAL OF POWER SOURCES
www.elsevier.com/locate/jpowsour

Electrode kinetics of ethanol oxidation on novel CuNi alloy supported catalysts synthesized from PTFE suspension

S. Sen Gupta, J. Datta *

Department of Chemistry, Bengal Engineering and Science University, Shibpur, Howrah 711103, India

Accepted 28 January 2005
Available online 31 May 2005

Abstract

An understanding of the kinetics and mechanism of the electrochemical oxidation of ethanol is of considerable interest for the optimization of the direct ethanol fuel cell. In this paper, the electro-oxidation of ethanol in sodium hydroxide solution has been studied over 70:30 CuNi alloy supported binary platinum electrocatalysts. These comprised mixed deposits of Pt with Ru or Mo. The electrodepositions were carried out under galvanostatic condition from a dilute suspension of polytetrafluoroethylene (PTFE) containing the respective metal salts. Characterization of the catalyst layers by scanning electron microscope (SEM)–energy dispersive X-ray (EDX) indicated that this preparation technique yields well-dispersed catalyst particles on the CuNi alloy substrate. Cyclic voltammetry, polarization study and electrochemical impedance spectroscopy were used to investigate the kinetics and mechanism of ethanol electro-oxidation over a range of NaOH and ethanol concentrations. The relevant parameters such as Tafel slope, charge transfer resistance and the reaction orders in respect of OH^- ions and ethanol were determined.

Keywords: Direct ethanol fuel cell; CuNi alloy; Polytetrafluoroethylene; Ethanol electro-oxidation; Reaction order; Charge transfer resistance

1. Introduction

In recent years, interest in the development of direct alcohol fuel cell (DAFC) has considerably increased due to its advantages compared with other fuel cell systems such as easy fuel delivery and storage, no need for reforming and favorable power capability [1]. Numerous studies deal with the direct oxidation of methanol on platinum in acid media. Pt is the best anode for hydrogen oxidation, but in the presence of methanol, CO_{ads}, formed as a reaction intermediate, irreversibly adsorbs on the platinum surface, rapidly lowering its activity [2,3]. To overcome this problem, alloys of Pt with more oxophilic elements have been investigated as methanol electro-oxidation catalysts [4–9]. PtRu bifunctional catalysts are presently the most active for methanol oxidation, with Ru believed to serve the role of removing CO_{ads} as CO_2:

$$\text{Ru–OH} + \text{Pt–CO} \rightarrow \text{Ru} + \text{Pt} + \text{CO}_2 + \text{H}^+ + \text{e}^-$$

The search for efficient and inexpensive catalyst materials is a challenging problem, especially for the DMFC where a relatively high catalyst loading is still required. Pt and other noble metals, which are typically used as catalysts, is one of the major factors for cell costs.

Moreover, methanol has some particular disadvantages, e.g. it is relatively toxic, inflammable with a low boiling point and it is not a primary fuel. Therefore, other alcohols are being considered as alternative fuels [10–13]. Ethanol is an attractive fuel since it can be easily produced in large amount by the fermentation of sugar-containing raw materials from agriculture. The use of alcohols with longer chains for applications in fuel cells can also be attractive considering the higher energy content of the fuel [1].

Despite all efforts devoted to the development of DAFC, there still remain problems to be overcome in terms of efficiency and power density. In acidic systems, which constitute the majority of DMFCs, this results from a combination of

* Corresponding author. Tel.: +91 33 2668 4561; fax: +91 33 2668 4564.
E-mail address: jayatids@hotmail.com (J. Datta).

0378-7753/$ – see front matter © 2005 Elsevier B.V. All rights reserved.
doi:10.1016/j.jpowsour.2005.01.066

slow kinetics of methanol electro-oxidation at the anode and the permeation of methanol through the Nafion membrane that results in a depolarizing reaction at the cathode [14]. Use of alkaline media can significantly reduce the amount of adsorbed CO on platinum electrode because of the weaker bonding of the chemisorbed intermediates than in acidic media [15]. Among the other advantages of alkaline solution are wider selection of electrode materials and improved efficiency of the oxygen cathode.

We have been working with 70:30 copper–nickel alloy as substrate for fabricating the anode component of a DAFC. In the pervious paper [16], ethanol electro-oxidation on CuNi alloy supported electrocatalysts has been investigated. It was observed that the reaction activity of catalyst layers synthesized from PTFE suspension of noble metal salts was significantly higher. This was attributed to the better dispersion of catalyst particles from PTFE. The kinetics of methanol oxidation has been extensively studied in both acid [17] as well as alkaline [18] media. This work involves the investigation of ethanol oxidation in sodium hydroxide medium over electro-codeposited PtRu and PtMo on 70:30 CuNi alloy substrate from the kinetic and mechanistic point of view. Cyclic voltammetry, polarization measurements and electrochemical impedance spectroscopy were used to analyze the electro-oxidation process.

2. Experimental

2.1. Preparation of electrocatalysts

The 70:30 CuNi alloy material comprised plate of 1.0 mm thickness from which specimens of appropriate size were cut. The binary catalysts were codeposited onto the CuNi alloy substrate by the electroreduction of the corresponding metal salts at a constant current density of 15 mA cm^{-2}. The deposition process was carried out in an aqueous solution containing 2% (w/w) of PTFE emulsion and the following metal salts: 5×10^{-2} M $H_2PtCl_6 \cdot 6H_2O$ (Arora Matthey Ltd.) and 2.5×10^{-1} M of the second metal salt ($RuCl_3 \cdot 3H_2O$, Arora Matthey Ltd. and $Na_2MoO_4 \cdot 2H_2O$, E. Merck (India) Ltd.). The catalyst loading, controlled at 2 mg cm^{-2}, was determined by the mass difference of the substrate before and after deposition.

The surface morphology of the electrocatalysts was investigated with a LEO S 430i scanning electron microscope (SEM) at an accelerating potential of 20 kV. The chemical composition of the catalyst layers was determined by energy dispersive X-ray (EDX) using Link ISIS EDX detector (Oxford Instruments, U.K.) coupled with the scanning electron microscope.

2.2. Electrochemical measurements

Electrochemical measurements were conducted using a computer controlled potentiostat/galvanostat with PG STAT 12 and FRA modules (Ecochemie B.V., The Netherlands). A conventional H-type glass cell with a platinum foil counter electrode and a mercury–mercuric oxide reference electrode (MOE) (0.14 V versus SHE) was used for all electrochemical experiments. Potentials in this paper are expressed relative to mercury–mercuric oxide electrode. The geometrical area of the electrocatalyst exposed to the solution was always 0.65 cm^{-2}. Nitrogen gas (XL grade from BOC India Ltd.) was bubbled in the NaOH supporting electrolyte for 15 min before starting each electrochemical experiment. All test solutions were prepared using triple distilled water.

Ethanol (AR grade, Merck) was added to the nitrogen saturated sodium hydroxide solution to obtain the required concentration of the alcohol. Cyclic voltammograms of ethanol electro-oxidation were recorded between −1.0 to 0.5 V at a sweep rate of 50 mV/s. Linear sweep voltammograms obtained at a slow sweep rate of 1 mV/s afforded the determination of the reaction order with respect to NaOH and ethanol concentrations. Steady state potentiostatic data were recorded after polarisation for 5 min.

For electrochemical impedance measurements, prior to the addition of ethanol to the electrolyte, the surface of the working electrode was cleaned electrochemically by cycling the potential between −1.0 to 0.5 V at 50 mV s^{-1} in 0.5 M NaOH until the cyclic voltammogram stopped changing. After injection of ethanol, the potential of the electrode was stepped to the desired value. Allowing 30 s for equilibration, impedance at each measurement potential was obtained between 100 kHz and 15 mHz containing 80 data points.

3. Results and discussion

3.1. SEM–EDX analysis

During the course of electrodeposition of the noble metals on CuNi alloy substrate, it is to be considered that the reduction potentials of the metal salt precursors are in the order [19]:

$$PtCl_6^{2+}/Pt > Ru^{3+}/Ru \gg MoO_4^{2-}/Mo$$

Therefore, we expect the reduction of the Pt metal precursor to be more effective than either of the cometal precursors during constant current deposition of binary PtRu and PtMo catalysts. This has been confirmed by the results of the EDX analysis (Table 1). For the CuNi/PtRu(PTFE) electrocatalyst, the SEM image (Fig. 1a) show homogeneously distributed

Table 1
Results of EDX analysis of CuNi/PtRu(PTFE) and CuNi/PtMo(PTFE) catalysts

Catalyst	Elemental composition		
	%Pt	%Ru	%Mo
CuNi/PtRu(PTFE)	85	15	–
CuNi/PtMo(PTFE)	93	–	7

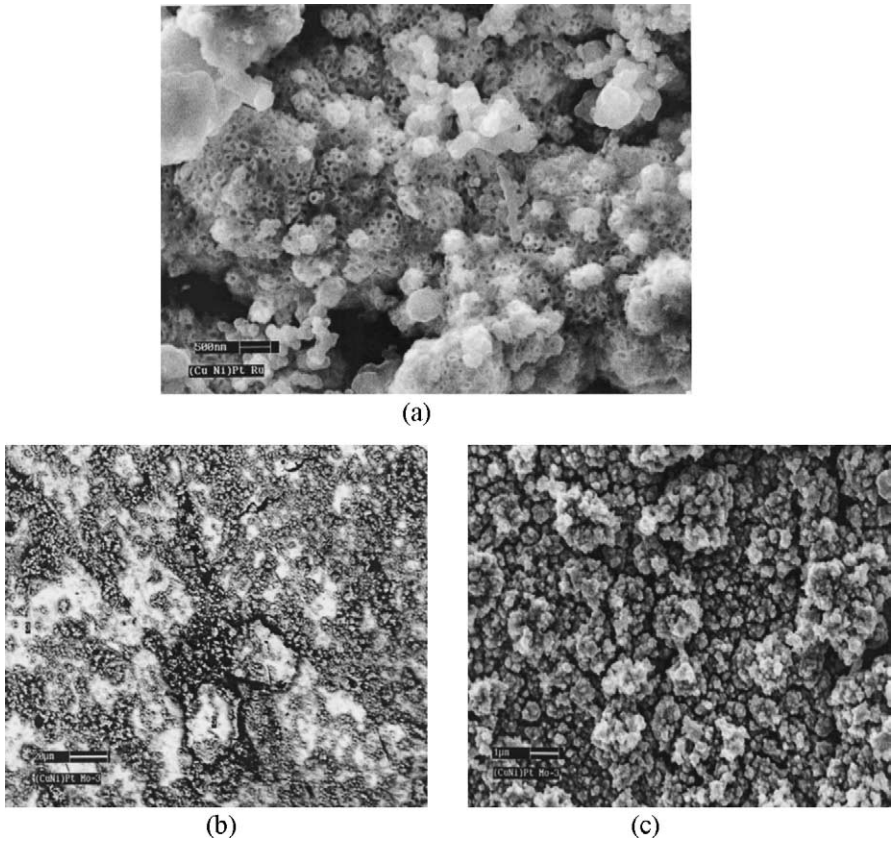

Fig. 1. SEM images of CuNi/PtRu(PTFE) (a) and CuNi/PtMo(PTFE) at two different magnifications (b and c).

small dark particles of about 50 nm in diameter, which we attribute to Ru codeposited with Pt on the catalyst surface as confirmed by EDX. Fig. 1b shows the SEM micrograph of CuNi/PtMo(PTFE) with the catalyst particles represented as gray regions on the CuNi alloy support (dark background). The EDX analysis of such particles distinguishes the presence of molybdenum and platinum, with an atomic ratio of 7% molybdenum and 93% platinum. The bright regions of the micrograph consist essentially of platinum deposits. A layer of well-dispersed catalyst particles is clearly visible in the SEM micrograph obtained at a higher magnification (Fig. 1c).

3.2. Ethanol oxidation in alkaline solution

3.2.1. Cyclic voltammetry and steady state polarisation studies

The cyclic voltammograms of CuNi/PtRu(PTFE) and CuNi/PtMo(PTFE) in 0.5 M NaOH (Fig. 2) are characterized by the well-known hydrogen adsorption/desorption features. These are followed by a small double layer charging/discharging region and the subsequent formation and reduction of surface oxides. For PtMo surfaces, an additional redox process in 0.5 M H_2SO_4 has been widely reported [20,21]. This is usually attributed to MoO_2/MoO_3 redox couple. The presence of the redox process at about −0.75 V for CuNi/PtMo(PTFE) in 0.5 M NaOH is most likely due to this $Mo^{4+} \leftrightarrow Mo^{6+}$ oxidation state change of Mo.

In presence of 1.0 M ethanol, a broad ethanol oxidation peak appears for CuNi/PtRu(PTFE) in the potential region −250 to 250 mV. The onset potential of ethanol oxidation was approximately −750 mV. As is evident, in the course of multiple scanning there is very little change in the overall nature of the CV. Notably, the peak current remains unchanged from the 1st to the 50th scan reflecting little poisoning of the catalyst surface. The one distinguishing feature in the ethanol oxidation behavior of CuNi/PtMo(PTFE) (Fig. 2b) is the near constant current of 0.07 A obtained at potentials more positive than −250 mV. In effect, there is no well-defined peak in the anodic as well as the cathodic sweep of the cyclic voltammogram.

Fig. 3 shows the anodic polarisation curves for ethanol oxidation at room temperature. It is evident that the polarisation curves have linear Tafel portions in the potential range of ca. −0.7 to −0.55 V. In this region, the CuNi/PtMo(PTFE) electrode shows a higher activity towards ethanol electrooxidation. But at more positive electrode potentials the activity of the Pt–Ru system increases in relation to Pt-Mo catalyst surface. The chronoamperometric curves recorded at −0.1 V (Fig. 4) show that overall there is a drop in current density with time for both the electrocatalysts. The behavior at short times is illustrated in the inset of Fig. 4. Initially, the Pt-

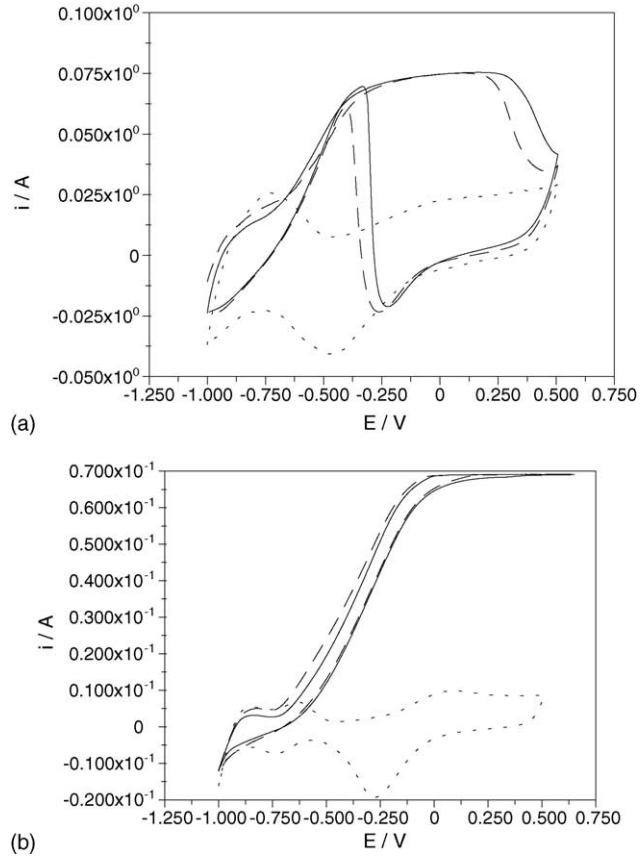

Fig. 2. Cyclic voltammograms on (a) CuNi/PtRu(PTFE), (b) CuNi/PtMo(PTFE) in 0.5 M NaOH without (- - -) and with 1.0 M ethanol (– – –) first scan, (—) 50th scan. Sweep rate: 50 mV s^{-1}.

Mo surface exhibits a higher electrocatalytic activity towards ethanol oxidation. However, over longer periods of time the activity of the Pt-Mo catalyst diminishes in relation to Pt–Ru. Therefore the current–time transients provides evidence for

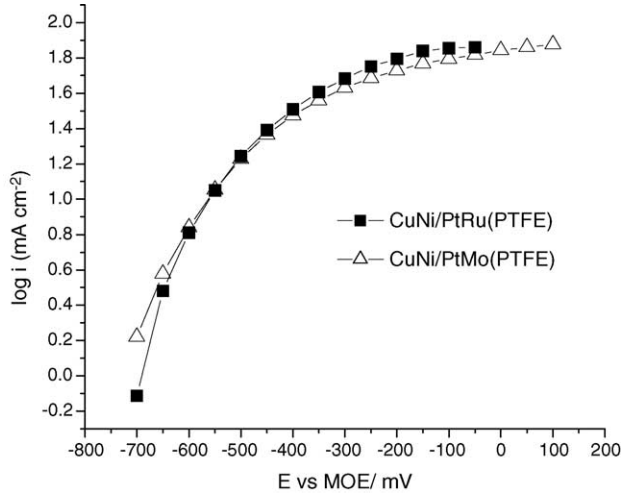

Fig. 3. Potentiostatic polarisation curves for ethanol (1.0 M) oxidation in 0.5 M NaOH.

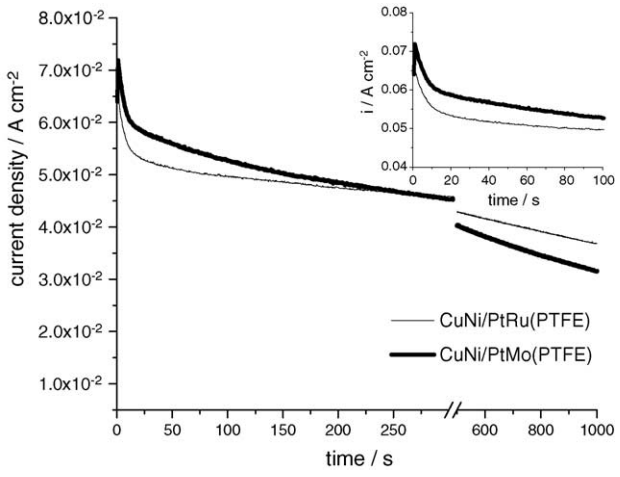

Fig. 4. Chronoamperometric curves recorded at −100 mV in 0.5 M NaOH and 1.0 M ethanol for the comparison of the electrodes' activity towards ethanol oxidation.

the faster deactivation of the Pt-Mo electrocatalyst than what is observed for the Pt–Ru system.

3.2.2. *Effect of NaOH concentration on ethanol oxidation*

The effect of NaOH concentration on ethanol electro-oxidation on CuNi/PtRu(PTFE) and CuNi/PtMo(PTFE) is depicted in Fig. 5, which shows a clear enhancement in the oxidation reaction with increasing pH. This fact suggests that the kinetics of ethanol electro-oxidation are enhanced by the greater availability of OH^- ions in solution, and hence, a higher OH^- coverage on the electrode surface.

A linear region for about 150 mV of the electrode potential describes the Tafel plots (Fig. 6) corresponding to the quasi-steady state curves obtained at a slow sweep rate of 1 mV s^{-1}. For NaOH concentrations greater than 0.5 M, an identical Tafel slope of 123 mV dec^{-1} for CuNi/PtRu(PTFE) and 129 mV dec^{-1} for CuNi/PtMo(PTFE) was obtained. This suggests that the same reaction mechanism occurs throughout this pH range. Below 0.5 M NaOH, the Tafel slope increased with decreasing NaOH concentration possibly resulting from the lower reactivity towards ethanol oxidation.

The plots illustrating the dependence $\log i$ versus $\log[OH^-]$ (Fig. 7), at several constant potentials from a region where the quasi-steady state curves obey the Tafel equation show a reaction order of approximately 0.5 and 0.8 with respect to OH^- species for CuNi/PtRu(PTFE) and CuNi/PtMo(PTFE), respectively.

3.2.3. *Effect of ethanol concentration*

Fig. 8 shows the effect of ethanol concentration on the quasi-steady state curves for ethanol oxidation on CuNi/PtRu(PTFE) and CuNi/PtMo(PTFE) at a fixed NaOH concentration of 0.5 M. It is clearly observed that at lower concentration levels the anodic current increases with increasing ethanol concentration, indicating that the reaction

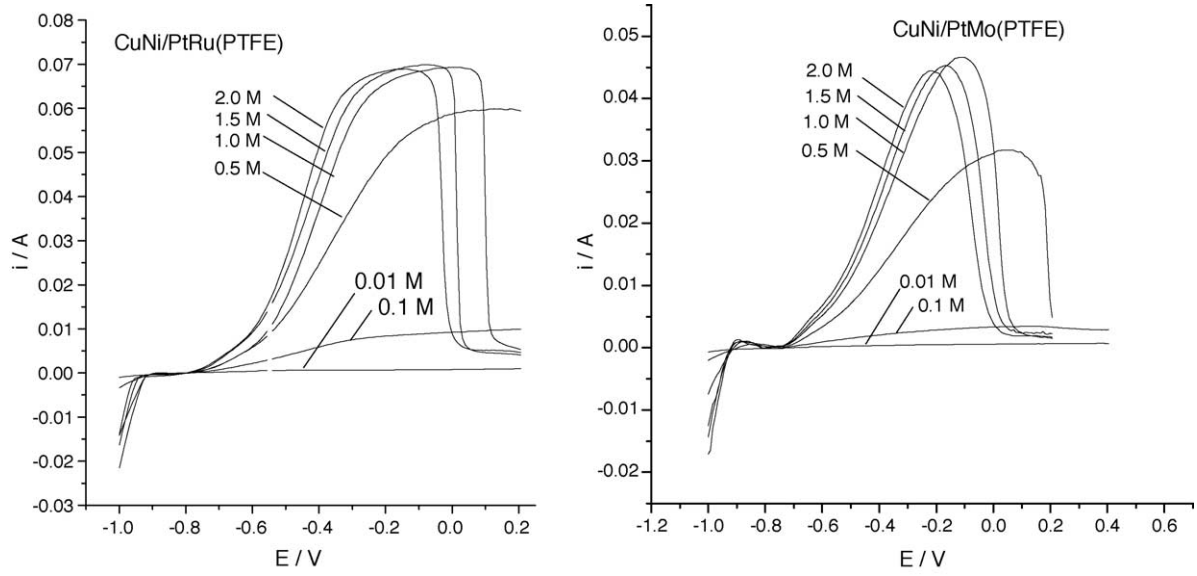

Fig. 5. Linear sweep voltammograms for ethanol oxidation on CuNi/PtRu(PTFE) and CuNi/PtMo(PTFE) in 1.0 M ethanol at various NaOH concentrations. Sweep rate: 1 mV s^{-1}.

was controlled by ethanol concentration at the electrode surface. The anodic peak current falls off at ethanol concentrations higher than 1.0 M. We assume this effect to be due to depletion of OH^- at the electrode surface. Therefore, it can be concluded that at lower ethanol concentrations, the peak currents in the voltammograms were controlled by the diffusion transport of ethanol due to the excess availability of OH^- ions. At higher ethanol concentrations, peak currents in the voltammograms were controlled by the diffusion transport of OH^- ions because of the excess availability of ethanol and insufficient OH^- ions.

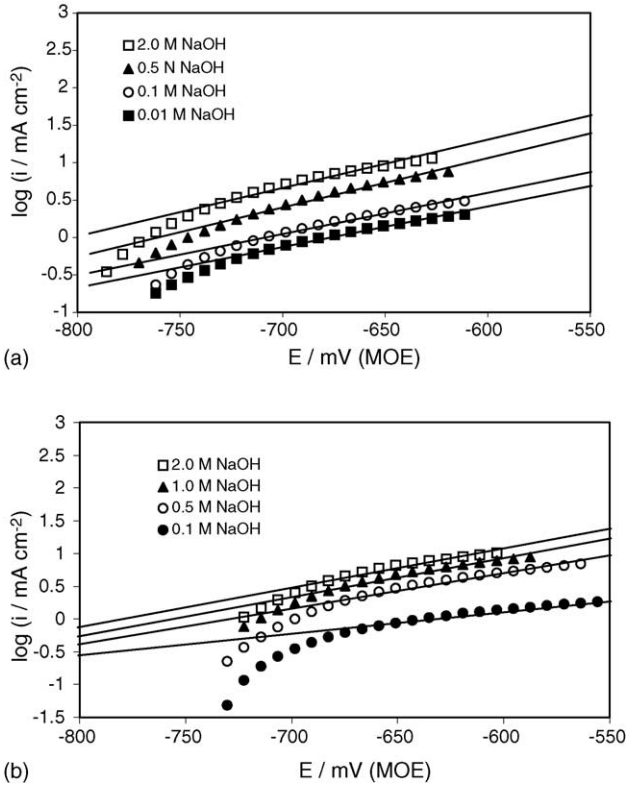

Fig. 6. Tafel plots for the oxidation of 1.0 M ethanol on (a) CuNi/PtRu(PTFE) and (b) CuNi/PtRu(PTFE) at various NaOH concentrations. Sweep rate: 1 mV s^{-1}.

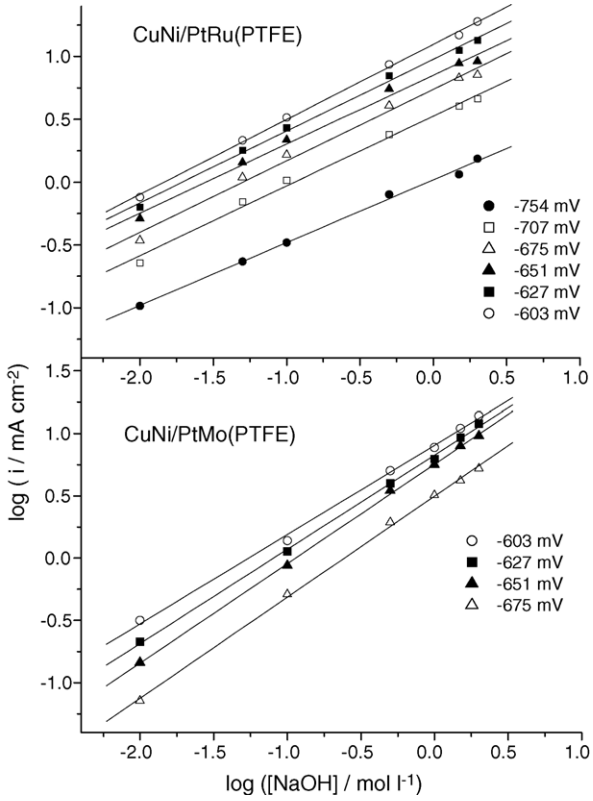

Fig. 7. Relation between ethanol oxidation rate with OH^- concentration in 1.0 M ethanol.

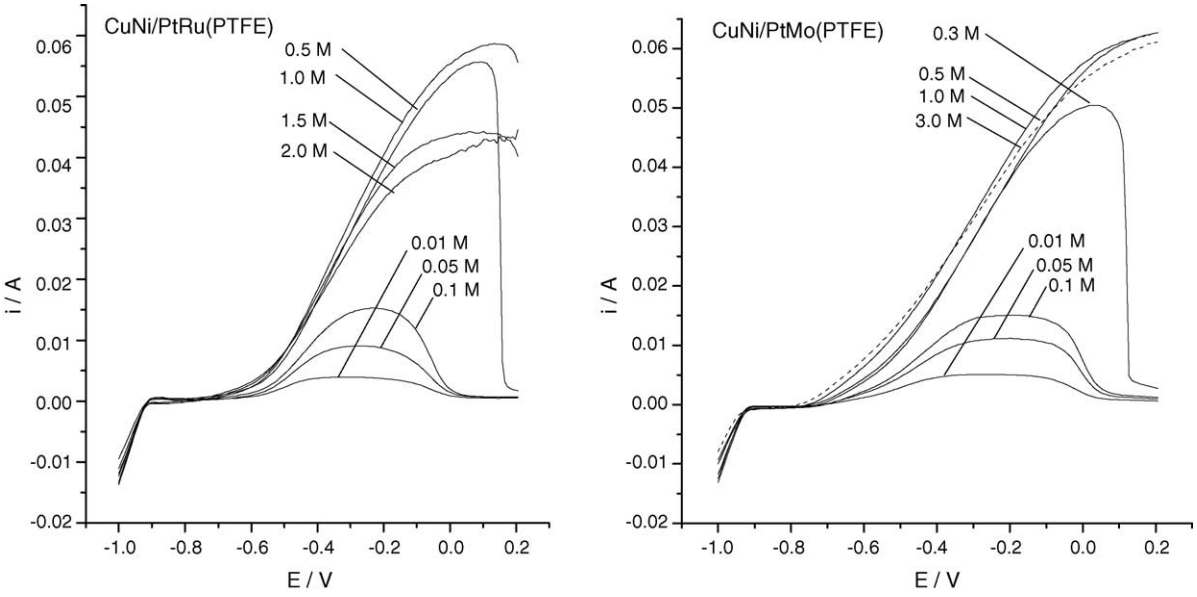

Fig. 8. Linear sweep voltammograms for ethanol oxidation on CuNi/PtRu(PTFE) and CuNi/PtMo(PTFE) in 0.5 M NaOH at various ethanol concentrations. Sweep rate: 1 mV s^{-1}.

Tafel plots for the ethanol oxidation reaction for a range of ethanol concentrations are given in Fig. 9. At ethanol concentrations between 1.0 and 0.1 M, the Tafel slopes for the CuNi/PtMo(PTFE) electrode were almost identical. The Tafel slope in this range was 132 mV dec^{-1}, although this increased to 153 mV dec^{-1} in 0.01 M ethanol. For the CuNi/PtRu(PTFE) electrode, a Tafel slope value of 141 mV dec^{-1} was obtained for ethanol concentrations above 0.1 M. The reaction order for ethanol, obtained from the slope of the log *i* versus log[EtOH] plot (Fig. 10) was more or less independent of the potential within the Tafel potential range (Table 2).

It is clear that at low potentials reaction orders for OH^- and EtOH are higher for the PtMo system as compared to the PtRu electrocatalyst. In the present study, it is probable that the differences are related to the formation of oxygenated species at low potentials. X-ray absorption studies indicate the presence of oxide layers on PtMo for potential as low as 0.1 V (versus RHE) in H_2SO_4 [22]. Oxidation of reaction intermediates resulting from the dissociative absorption of ethanol requires surface bound hydroxyl species [23]. A higher order for EtOH at the PtMo electrode implies a higher concentration of ethanol residues at this surface. The presence

Table 2
Reaction orders with respect to OH and ethanol for CuNi/PtRu(PTFE) and CuNi/PtMo(PTFE) catalysts

Potential (mV) (vs. MOE)	CuNi/PtRu(PTFE)		CuNi/PtMo(PTFE)	
	OH^-	EtOH	OH^-	EtOH
−651	0.55	0.27	0.80	0.37
−603	0.59	0.27	0.72	0.35
−500	0.61	0.26	0.74	0.31

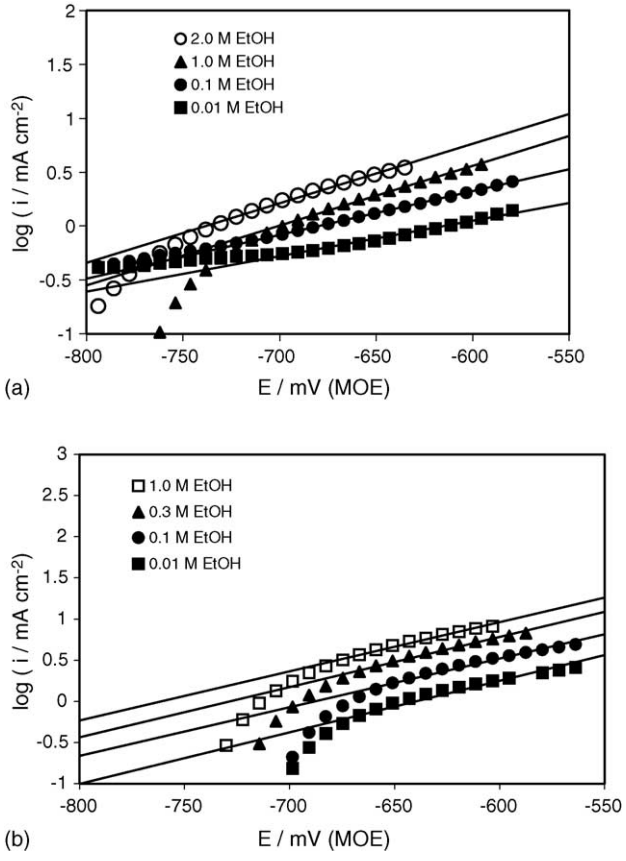

Fig. 9. Tafel plots for ethanol oxidation of 0.5 M NaOH on (a) CuNi/PtRu(PTFE) and (b) CuNi/PtMo(PTFE) at various ethanol concentrations. Sweep rate: 1 mV s^{-1}.

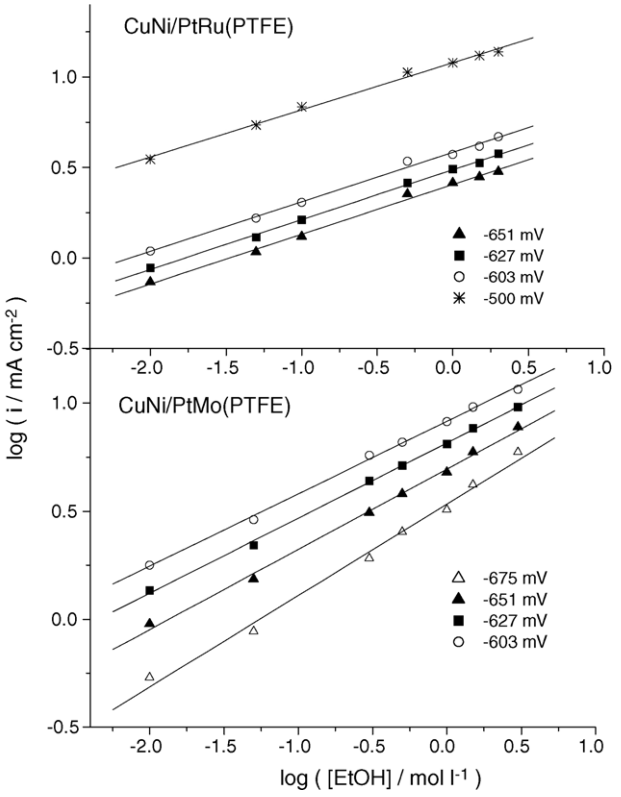

Fig. 10. Dependence of ethanol oxidation rate on ethanol concentration in 0.5 M NaOH.

of Mo leads to the formation on its surface of OH_{ads} species, which promotes the oxidative removal of the adsorbed intermediates on Pt at low potentials. It may be speculated that the ability of Ru to supply oxygen-like species is inferior to that of Mo at these potentials. This is reflected in its lower reaction orders with respect to OH^- and EtOH as compared to the PtMo electrocatalyst.

3.3. Electrochemical impedance spectroscopy (EIS)

The charge transfer resistance R_{ct}, as measured by the diameter of the semi-circle in a Nyquist plot, is related to the charge transfer reaction kinetics according to the following equation [24]:

$$R_{ct} = \frac{RT}{nFi_0} \quad (1)$$

where

$$i_0 = nFAk_0 C_0^{*(1-\alpha)} C_R^{*\alpha} \quad (2)$$

R is molar gas constant ($J\,mol^{-1}\,K^{-1}$), T temperature (K), n number of electrons transferred, F Faraday constant (C), i_0 exchange current (A), A reaction area (cm^2), k_0 standard heterogeneous rate constant ($cm\,s^{-1}$), C_0^*, C_R^* bulk concentration of oxidation and reduction species ($mol\,l^{-1}$) and α is transfer coefficient.

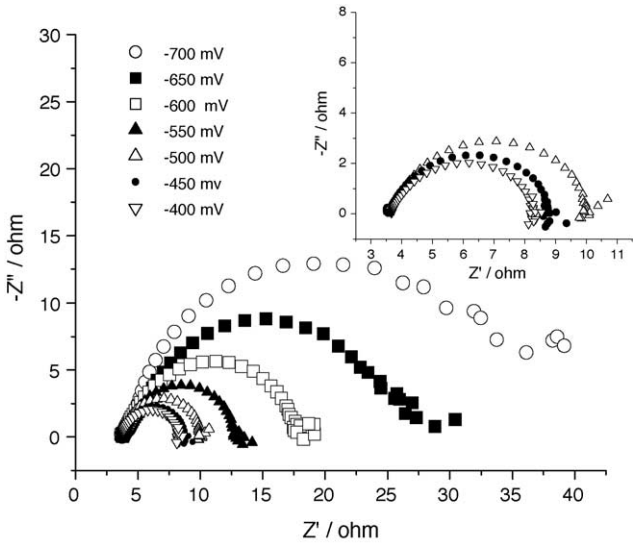

Fig. 11. Nyquist plots for ethanol oxidation CuNi/PtMo(PTFE) at different potentials in 1.0 M ethanol and 0.5 M NaOH.

Nyquist plots for ethanol electro-oxidation on CuNi/PtMo(PTFE) in 1.0 M ethanol/0.5 M NaOH are shown in Fig. 11. In the potential region −700 to −100 mV, the Nyquist plots show a semi-circle, which can be assigned to a kinetically controlled reaction. The charge transfer resistance decreased with increasing potential indicating an increase in reaction kinetics at higher potentials. The same relation between R_{ct} and potential was also observed for the CuNi/PtRu(PTFE) electrode.

Fig. 12 shows Nyquist plots for ethanol oxidation on CuNi/PtRu(PTFE) at −600 mV for a range of NaOH concentrations from which it is clear that the solution and charge transfer resistance decreased as the NaOH concentration increased. This indicates that the reaction activity increased with increasing NaOH concentration, which is in agreement with the linear sweep voltammograms. A comparison

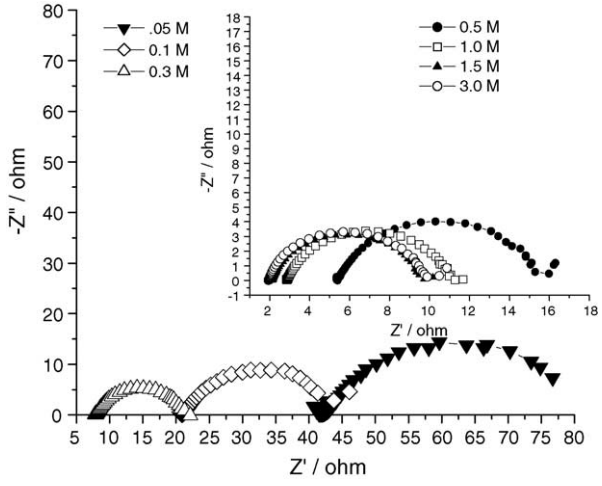

Fig. 12. Impedance spectra for ethanol oxidation on CuNi/PtRu(PTFE) in 1.0 M ethanol with various concentrations of NaOH at −600 mV.

Table 3
Charge transfer resistance (R_{ct}) for ethanol oxidation at various NaOH and ethanol concentrations

Catalysts	Charge transfer resistance, R_{ct} (Ω)					
	1.0 M EtOH + different [NaOH]			0.5 M [NaOH] + different [EtOH]		
	0.1 M	0.5 M	1.5 M	0.1 M	0.5 M	1.5 M
CuNi/PtRu(PTFE)	25.1	10.2	7.7	33.9	22.3	12.8
CuNi/PtMo(PTFE)	48.5	19.2	18.3	87.0	52.0	32.2

of the dependence of the R_{ct} values on NaOH concentration for CuNi/PtRu(PTFE) and CuNi/PtMo(PTFE) is given in Table 3. At all NaOH concentrations, the resistance to charge transfer for the PtMo surface is higher than that for the PtRu catalyst. The effect of ethanol concentration on the impedance response in 0.5 M NaOH for CuNi/PtRu(PTFE) electrode is shown in Fig. 13. The Nyquist plots, obtained at a constant potential of −600 mV, indicate a charge transfer resistance that decreased with increasing ethanol concentration up to 1.0 M. This behavior suggests that the reaction kinetics were promoted by the adsorption of ethanol on the electrode surface. Beyond an ethanol concentration of 1.0 M, R_{ct} values remained almost constant. We assume this to be due to either the saturation of active sites or depletion of OH^- at the surface of the electrode.

The charge transfer resistance at CuNi/PtMo(PTFE) is consistently higher than at the CuNi/PtRu(PTFE) electrode at all combinations of NaOH and EtOH concentrations studied. This is presumably because of the sluggish nature of the rate of charge transfer across the PtMo electrode/electrolyte interface. Without the effect of difference in the coverage of reaction intermediates, the charge transfer resistance depends on kinetic parameters [25]. The slow kinetics of charge transfer process at PtMo surface may arguably lead to the buildup of ethanol reaction intermediate, which would inhibit further adsorption of ethanol.

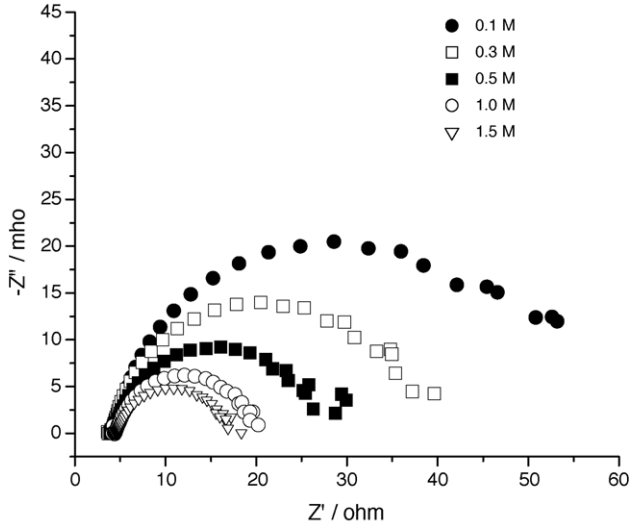

Fig. 13. Impedance spectra for ethanol oxidation on CuNi/PtRu(PTFE) in 0.5 M NaOH with various concentrations of ethanol at −600 mV.

4. Conclusion

Electro-codeposition of platinum–ruthenium and platinum–molybdenum on CuNi alloy substrate from PTFE suspension provides a novel route of synthesizing well-dispersed Pt based binary catalysts. The CuNi/PtMo(PTFE) electrode has shown enhanced performance compared to CuNi/PtRu(PTFE) at low potentials. The ability of the Mo modified electrocatalyst to transfer oxygenated species at lower electrode potentials is explained as the cause for its higher reaction orders with respect to both NaOH and ethanol. However, the charge transfer resistance across this catalytic surface is higher than that observed for CuNi/PtRu(PTFE). The slow kinetics of charge transfer process at PtMo surface may lead to the buildup of ethanol reaction intermediate, which would inhibit further adsorption of ethanol. This has been demonstrated by the faster rate of deactivation of the PtMo surface than what is observed for the PtRu system during the chronoamperometric study.

Acknowledgement

We gratefully acknowledge the financial support by the Defence Research and Development Organization (DRDO), New Delhi, India.

References

[1] C. Lamy, A. Lima, V. LeRhun, F. Delime, C. Coutanceau, J.-M. Leger, J. Power Sources 105 (2002) 283.
[2] S. Wilhelm, T. Iwasita, W. Vielstich, J. Electroanal. Chem. 238 (1987) 383.
[3] T.R. Ralph, M.P. Hogarth, Platinum Met. Rev. 46 (2002) 117.
[4] M. Watanabe, S. Motoo, J. Electroanal. Interfacial Electrochem. 60 (1975) 267.
[5] M.M.P. Jansenn, J. Moolhuysen, Electrochim. Acta 21 (1976) 861.
[6] H.A. Gasteiger, N.M. Markovic, P.N. Ross Jr., J. Phys. Chem. 97 (1993) 12020.
[7] H. Hoster, T. Iwasita, H. Baumgartner, W. Vielstich, Phys. Chem. Chem. Phys. 3 (2001) 337.
[8] U. Koponen, H. Kumpulainen, M. Berglin, J. Keskineu, T. Peltoneu, M. Valkiaineu, M. Wasberg, J. Power Sources 118 (2003) 325.
[9] Z. Jusys, T.J. Schmidt, L. Dubau, K. Lasch, L. Jorissen, J. Garche, R.J. Behm, J. Power Sources 105 (2002) 297.
[10] C. Lamy, E.M. Belgsir, J.-M. Leger, J. Appl. Electrochem. 31 (2001) 799.
[11] E. Peled, T. Duvdevani, A. Aharon, A. Melman, Electrochem. Solid State Lett. 4 (2001) 38.

[12] D. Cao, S.H. Bergens, J. Power Sources 124 (2003) 12.
[13] Z. Qi, A. Kaufman, J. Power Sources 118 (2003) 54.
[14] S. Wasmus, A. Kuver, J. Electroanal. Chem. 461 (1999) 14.
[15] B. Beden, J.M. Leger, C. Lamy, in: J.O'M. Bockris, B.E. Conway, R.E. White (Eds.), Modern Aspects of Electrochemistry, vol. 22, Plenum Press, New York, 1992.
[16] S. Sen Gupta, J. Datta, J. Power Sources 131 (2004) 169.
[17] O.A. Khazova, A.A. Mikhailova, A.M. Skundin, E.K. Tuseeva, A. Havranek, K. Wippermann, Fuel Cells 2 (2002) 99.
[18] E.H. Yu, K. Scott, R.W. Reeve, L. Yang, R.G. Allen, Electrochim. Acta 49 (2004) 2443.
[19] W.M. Latimer, The Oxidation States of the Elements and their Potentials in Aqueous Solutions, second ed., Prentice-Hall, Inc., 1961.
[20] Y. Wang, E.R. Fachini, G. Curz, Y. Zhu, Y. Ishikanse, J.A. Colucei, C.R. Cabrera, J. Electrochem. Soc. 148 (2001) 222.
[21] A.L.N. Pinheiro, A. Oliveira-Neto, E.C. de Souza, J. Perez, V.A. Pganin, E.A. Ticianelli, E.R. Gonzalez, J. New Mater. Electrochem. Syst. 6 (2003) 1.
[22] S. Mukerjee, S. Lee, E.A.Q. Ticianelli, J. McBreen, B.N. Grgur, N.M. Markovic, P.N. Ross, J.R. Giallombardop, E.S. De Castro, Electrochem. Solid State Lett. 2 (1999) 12.
[23] T. Iwasita, Third LAMNET Workshop Proceedings, Brazil, 2002.
[24] A.J. Bard, L.R. Faulkner, Electrochemical Methods, John Wiley & Sons, 1980.
[25] R.E. Melnick, G.T.R. Palmore, J. Phys. Chem. B 105 (2001) 1012.